

Instability of agegraphic dark energy models

Kyoung Yee Kim, Hyung Won Lee and Yun Soo Myung*

*Institute of Mathematical Science and School of Computer Aided Science
Inje University, Gimhae 621-749, Korea*

Abstract

We investigate the agegraphic dark energy models which were recently proposed to explain the dark energy-dominated universe. For this purpose, we calculate their equation of states and squared speeds of sound. We find that the squared speed for agegraphic dark energy is always negative. This means that the perfect fluid for agegraphic dark energy is classically unstable. Furthermore, it is shown that the new agegraphic dark energy model could describe the matter (radiation)-dominated universe in the far past only when the parameter n is chosen to be $n > n_c$, where the critical values are determined to be $n_c = 2.6878(2.5137752)$ numerically. It seems that the new agegraphic dark energy model is no better than the holographic dark energy model for the description of the dark energy-dominated universe, even though it resolves the causality problem.

*e-mail address: ysmjung@inje.ac.kr

1 Introduction

Observations of supernova type Ia suggest that our universe is accelerating [1]. Considering the Λ CDM model [2, 3], the dark energy and cold dark matter contribute $\Omega_{\Lambda}^{\text{ob}} \simeq 0.74$ and $\Omega_{\text{CDM}}^{\text{ob}} \simeq 0.22$ to the critical density of the present universe. Recently the combination of WMAP3 and Supernova Legacy Survey data shows a significant constraint on the equation of state (EOS) for the dark energy, $w_{\text{ob}} = -0.97_{-0.09}^{+0.07}$ in a flat universe [4, 5].

Although there exist a number of dark energy models [6], the two promising candidates are the cosmological constant and the quintessence scenario [7]. The EOS for the latter is determined dynamically by the scalar or tachyon.

On the other hand, there exist interesting models of the dark energy which satisfy the holographic principle, especially the entropy bound. One is the holographic dark energy model [8] and the other is the agegraphic dark energy model [9]. The first is based on the energy bound $E_{\Lambda} \leq E_{BH} \rightarrow L^3 \rho_{\Lambda} \leq m_{\text{p}}^2 L$ [10, 11] with the length scale L ¹ (IR cutoff) of the universe, while the latter is based on the Károlyházy relation of $\delta t = \lambda t_{\text{p}}^{2/3} t^{1/3}$ [12, 13, 14] and the time-energy uncertainty of $E_{\delta t^3} \sim t^{-1}$ in the Minkowski spacetime, giving $\rho_{\text{q}} \sim \frac{E_{\delta t^3}}{(\delta t)^3} \sim \frac{m_{\text{p}}^2}{t^2}$ [15]. Hence we find the vacuum energy density $\rho_{\Lambda} = 3c^2 m_{\text{p}}^2 / L^2$ as the holographic dark energy density, whereas the energy density of metric perturbations $\rho_{\text{q}} = 3n^2 m_{\text{p}}^2 / T^2$ with the age of the universe $T = \int_0^t dt'$ as the agegraphic dark energy density. Here the undetermined parameters c and n are introduced to describe the appropriate dark energy model. It seems that the agegraphic dark energy model does not suffer the causality problem of the holographic dark energy model because the agegraphic dark energy model do not use the future event horizon. However, this model suffers from the contradiction to describe the matter-dominated universe in the far past. Hence, the new agegraphic dark energy model was introduced to resolve this issue [16].

The two important quantities for the cosmological evolution of the universe are the EOS $\omega = p/\rho$ and the squared speed of sound velocity $v_s^2 = dp/d\rho$. The first describes the nature of evolution and the latter determines the stability of evolution.

In general, it is not easy to determine the EOS for a cosmological model with the IR cutoff L . If one considers $L = H_0^{-1}$ together with the cold dark matter, the EOS may take the form of $w_{\Lambda} = 0$ [17], which is just that of the cold dark matter. Fortunately, choosing the future event horizon for the holographic dark energy model determines the accelerating universe when using the continuity equation [18].

One may consider the linear perturbation of holographic dark energy to test the sta-

¹Here, two length scales are introduced: the future event horizon $R_{\text{FH}} = a(t) \int_t^{\infty} \frac{dt'}{a(t')}$ and the particle horizon $R_{\text{PH}} = a(t) \int_0^t \frac{dt'}{a(t')}$ with the flat Friedmann-Robertson-Walker metric $ds_{\text{FRW}}^2 = -dt^2 + a^2(t) d\mathbf{x} \cdot d\mathbf{x}$.

bility of a dark energy-dominated universe. For this purpose, an important quantity is the squared speed v_s^2 of sound [19]. The sign of v_s^2 is crucial for determining the stability of a background evolution. If this is negative, it implies a classical instability of a given perturbation. It was shown that the Chaplygin gas (tachyon) have the positive squared speeds of sound with $v_{C,T}^2 = -\omega_{C,T}$ and thus they are supposed to be stable against small perturbations [20, 21]. However, the perfect fluid of holographic dark energy with future event horizon is classically unstable because its squared speed is always negative [22].

In this Letter, we investigate the agegraphic dark energy models including new agegraphic dark energy model by calculating their EOS ω_q and squared speed v_q^2 . We compare these agegraphic dark energy models with the holographic dark energy model. Especially, we show that the parameter n of the new agegraphic dark energy model is restricted to $n > n_c$, in order to describe the matter (radiation)-dominated universe in the far past.

2 Agegraphic dark energy model

2.1 Noninteracting case

In this section we discuss agegraphic dark energy model [9]. A flat universe composed of ρ_q and the cold dark matter ρ_m is governed by the Friedmann equation

$$H^2 = \frac{1}{3m_p^2}(\rho_q + \rho_m) \quad (1)$$

and their continuity equations

$$\dot{\rho}_q + 3H(\rho_q + p_q) = 0, \quad (2)$$

$$\dot{\rho}_m + 3H\rho_m = 0. \quad (3)$$

Introducing the density parameters $\Omega_i = \rho_i/3m_p^2 H^2$, then one finds

$$\Omega_q = \frac{n^2}{(HT)^2} \quad (4)$$

which implies that the Friedmann equation (1) can be rewritten as

$$\Omega_q + \Omega_m = 1. \quad (5)$$

Considering the age of the universe $T = \int_0^a \frac{da'}{H' a'}$, its pressure is determined solely by Eq.(2) with $x = \ln a$ [18]

$$p_q = -\frac{1}{3} \frac{d\rho_q}{dx} - \rho_q \quad (6)$$

which provides the EOS [9]

$$\omega_q = \frac{p_q}{\rho_q} = -1 + \frac{2}{3n} \sqrt{\Omega_q}. \quad (7)$$

Here ω_q is determined by the evolution equation

$$\Omega'_q = \frac{\dot{\Omega}_q}{H} = -3\omega_q \Omega_q (1 - \Omega_q) \quad (8)$$

where $'$ and $\dot{}$ are the derivative with respect to x and cosmic time t , respectively. For our purpose, we introduce the squared speed of agegraphic dark energy fluid as

$$v_q^2 = \frac{dp_q}{d\rho_q} = \frac{\dot{p}_q}{\dot{\rho}_q}, \quad (9)$$

where

$$\dot{p}_q = \dot{\omega}_q \rho_q + \omega_q \dot{\rho}_q \quad (10)$$

with

$$\dot{\omega}_q = H \frac{\Omega'_q}{3n\sqrt{\Omega_q}} = H\omega'_q. \quad (11)$$

It leads to

$$v_q^2 = -\frac{\dot{\omega}_q}{3H(1 + \omega_q)} + \omega_q = -\frac{\Omega'_q}{9n(1 + \omega_q)\sqrt{\Omega_q}} + \omega_q. \quad (12)$$

In the linear perturbation theory, the density perturbation is described by

$$\rho(t, \mathbf{x}) = \rho(t) + \delta\rho(t, \mathbf{x}) \quad (13)$$

with $\rho(t)$ the background value. Then the conservation law for the energy-momentum tensor of $\nabla_\nu T^{\mu\nu} = 0$ yields [23]

$$\delta\ddot{\rho} = v^2 \nabla^2 \delta\rho(t, \mathbf{x}), \quad (14)$$

where $T^0_0 = -\rho(t) - \delta\rho(t, \mathbf{x})$ and $v^2 = dp/d\rho$. For $v_q^2 > 0$, Eq. (14) becomes a regular wave equation whose solution is given by $\delta\rho_q = \delta\rho_{0q} e^{-i\omega t + i\mathbf{k}\cdot\mathbf{x}}$. Hence the positive squared speed (real value of speed) shows a regular propagating mode for a density perturbation. For $v_q^2 < 0$, the perturbation becomes an irregular wave equation whose solution is given by $\delta\rho_q = \delta\rho_{0q} e^{\omega t + i\mathbf{k}\cdot\mathbf{x}}$. Hence the negative squared speed (imaginary value of speed) shows an exponentially growing mode for a density perturbation. That is, an increasing density perturbation induces a lowering pressure, supporting the emergence of instability.

In the case of agegraphic dark energy model, one finds from Fig. 1 that the squared speed is always negative for the whole evolution $0 \leq \Omega_q \leq 1$. That is, we read off the

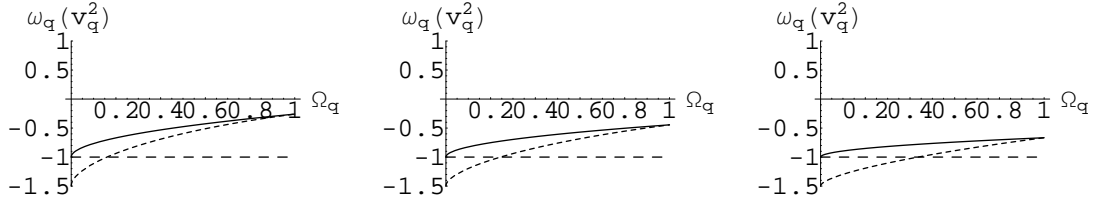


Figure 1: Graphs for the agegraphic dark energy model. The solid (dashed) lines denote the equation of state ω_q (squared speed v_q^2). One has three graphs for $n = 0.9$, $n = 1.2$, and $n = 2.0$ from the left to the right.

classical instability of $v_q^2 < 0$ for $-1 \leq \omega_q < 0$. Especially, even for $n = 0.9 (< 1)$, there is no phantom phase with $\omega_q < -1$, in contrast to the holographic dark energy model with the future event horizon [22]. Also there is no sizable difference between $n = 0.9, 1.2$ and 2.0 except slightly different loci for $v_q^2 = -1$. Furthermore, the EOS ω_q is a monotonically increasing function of Ω_q , which implies that one could not obtain the dark energy-dominated universe in the far future ($\Omega_q \rightarrow 1$, $\omega_q \rightarrow -1$).

2.2 Interacting case

We extend the agegraphic dark energy model to include the interaction with the cold dark matter through the continuity equations as

$$\dot{\rho}_q + 3H(\rho_q + p_q) = -Q, \quad \dot{\rho}_m + 3H\rho_m = Q, \quad (15)$$

which shows decaying of agegraphic dark energy density into the cold dark matter with decay rate $\Gamma = Q/\rho_q$. In this case, the evolution equation takes the form

$$\Omega'_q = \Omega_q \left[-3\omega_q(1 - \Omega_q) - \frac{Q}{3m_p^2 H^3} \right]. \quad (16)$$

Here we obtain the native equation of state [24, 25]

$$\omega_q = -1 + \frac{2}{3n} \sqrt{\Omega_q} - \frac{Q}{3H\rho_q}. \quad (17)$$

The squared speed is given by

$$v_q^2 = \frac{\omega'_q}{-3(1 + \omega_q^{\text{eff}})} + \omega_q, \quad (18)$$

where

$$\omega'_q = \frac{\Omega'_q}{3n\sqrt{\Omega_q}} - \left(\frac{Q}{3H\rho_q} \right)' \quad \text{and} \quad \omega_q^{\text{eff}} = \omega_q + \frac{Q}{3H\rho_q}. \quad (19)$$

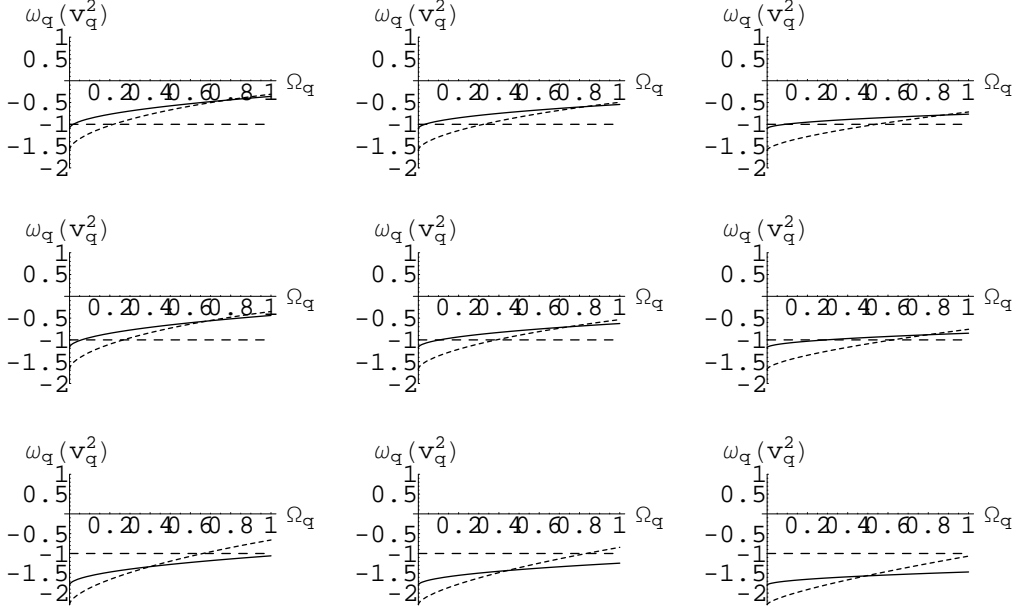


Figure 2: Nine graphs for the agegraphic dark energy. The solid (dashed) lines denote the native equation of state ω_q (squared speed v_q^2). From the left to the right, one has the graphs for $n = 0.9$, $n = 1.2$, and $n = 2$. From top to bottom, one has graphs for different $\alpha = 0.1, 0.18$ and $\alpha = 0.8$. There is no significant change between them.

If the decay rate is chosen to be $\Gamma = 3\alpha H$ with $\alpha \geq 0$, one finds a particular interaction. The evolution of the native EOS and the squared speed are shown in Fig. 2. It seems that all equation of states include the phantom phase with $\omega_q < -1$ as well as the negative squared speed for whole range of $0 \leq \Omega_q \leq 1$. However, it is unfair to say that the interaction can induce the phantom phase naturally [26]. In the case of interaction, we need to introduce the effective equation of state [27] to take into account the correct EOS as

$$\omega_q^{\text{eff}} = -1 + \frac{2}{3n} \sqrt{\Omega_q}. \quad (20)$$

In this case, the squared speed is given by

$$v_q^2 = \frac{(\omega_q^{\text{eff}})'}{-3(1 + \omega_q^{\text{eff}})} + \omega_q^{\text{eff}}, \quad (21)$$

where

$$(\omega_q^{\text{eff}})' = \frac{\Omega_q'}{3n\sqrt{\Omega_q}}. \quad (22)$$

The evolution of the effective EOS and the squared speed are shown in Fig. 3. All

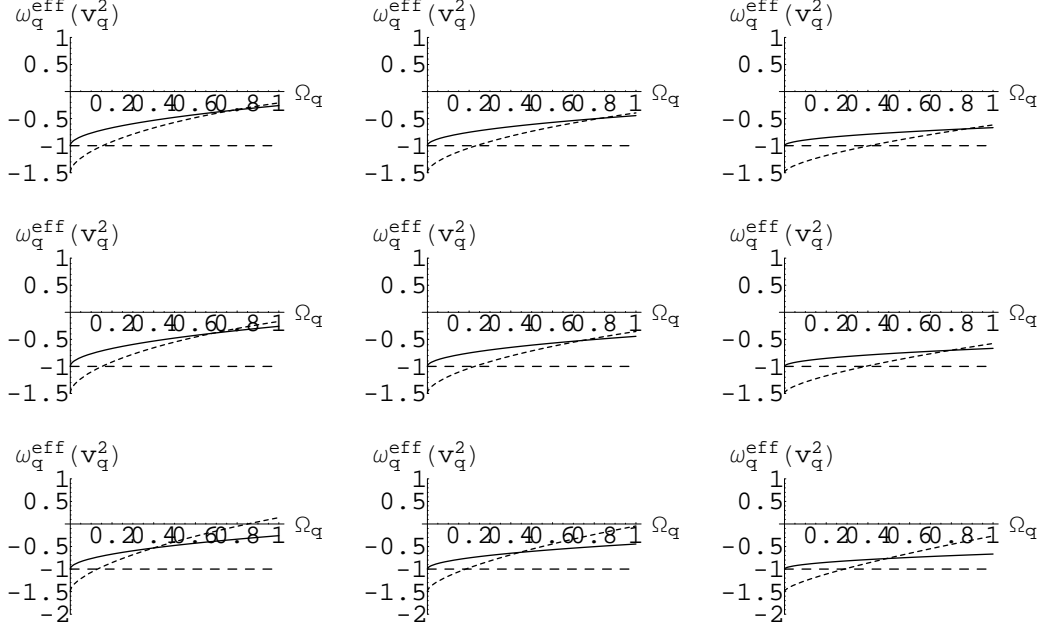


Figure 3: Nine graphs for the agegraphic dark energy. The solid (dashed) lines denote the effective equation of state ω_q^{eff} (squared speed v_q^2). From the left to the right, one has the graphs for $n = 0.9$, $n = 1.2$, and $n = 2$. From top to bottom, one has graphs for different $\alpha = 0.1, 0.18$ and $\alpha = 0.8$. There is no significant change between them.

equation of states are the non-phantom phase of $\omega_q^{\text{eff}} \geq -1$. We find that negative squared speeds appear for whole range of $0 \leq \Omega_q \leq 1$ except $n = 0.9$ and $\alpha = 0.8$. Hence the agegraphic dark energy model persists in having the negative squared speed, even for including the interaction with the cold dark matter.

2.3 Far Past behavior of $\Omega_q \rightarrow 0$

The agegraphic dark energy model has a drawback to describe the matter-dominated universe in the far past of $a \rightarrow 0$ and $\Omega_q \rightarrow 0$. From Eqs.(8) and (7), we have $\Omega_q \propto a^3$ and $\omega_q \rightarrow -1$. However, in the matter-dominated epoch, we have $a \propto t^{2/3}$ and thus $T^2 \propto a^3$. This means that $\rho_q \propto a^{-3}$ and $\omega_q \propto 0$. On the other hand, considering the Friedmann equation (1) with $\rho_m \propto a^{-3}$, we have $H^2 \propto a^{-3}$. This implies that $\Omega_q \propto \text{const}$, which contradicts to $\Omega_q \propto a^3$ in the far past. This inconsistency arises from the handicap of the agegraphic dark energy model. The issue is that $\omega_q \simeq 0$ is not predicted by the EOS in Eq.(7). This issue is similar to the holographic dark energy model when choosing $L_\Lambda = 1/H_0$ [17], where it may be resolved if introducing the interaction. Here, we have

to use the effective EOS given by $\omega_m^{\text{eff}} = -\frac{\Omega_a}{\Omega_m} \frac{Q}{3H\rho_q}$, instead of the native EOS ω_m . In this case, choosing an appropriate interaction Q may lead to $\omega_m^{\text{eff}} \rightarrow 0$ [28].

However, Wei and Cai have introduced the new agegraphic dark energy model to resolve the contradiction in the far past of agegraphic dark energy model [16].

3 New agegraphic dark energy model

In this section, we attempt to find the EOS and squared speed for the new agegraphic dark energy model [16]. This model is different from the agegraphic dark energy model by using the conformal time η instead of T

$$\eta = \int_0^t \frac{dt'}{a'} = \int_0^a \frac{da'}{(a')^2 H'}. \quad (23)$$

Then the corresponding energy density and its density parameter are given by

$$\rho_n = \frac{3n^2 m_p^2}{\eta^2}, \quad \Omega_n = \frac{n^2}{(H\eta)^2}. \quad (24)$$

3.1 Noninteracting case

The pressure is determined solely by Eq.(2)

$$p_n = -\frac{1}{3} \frac{d\rho_n}{dx} - \rho_n \quad (25)$$

which provides the EOS [29]

$$\omega_n = \frac{p_n}{\rho_n} = -1 + \frac{2}{3na} \sqrt{\Omega_n} = \frac{p_n}{\rho_n} = -1 + \frac{2e^{-x}}{3n} \sqrt{\Omega_n} \quad (26)$$

with $a = e^x$. ω_n is determined by the evolution equation

$$\Omega_n' = -3\omega_n \Omega_n (1 - \Omega_n). \quad (27)$$

Then, we introduce the squared speed of new agegraphic dark energy fluid as

$$v_n^2 = -\frac{\dot{\omega}_n}{3H(1+\omega_n)} + \omega_n = \frac{1}{2}(1-\Omega_n)w_n + w_n + \frac{1}{3}. \quad (28)$$

Considering Eq.(26) together with the condition $a \rightarrow 0$ ($x \rightarrow -\infty$) of the far past, the matter-dominated universe is recovered with $\omega_n = -2/3$ and $\Omega_n = n^2 a^2/4$, while the radiation-dominated universe is recovered with $\omega_n = -1/3$ and $\Omega_n = n^2 a^2$ [16]. However, this prediction comes from the EOS ω_n only. We remind the reader that the pictures

of far past and far future should be determined from Eq. (27) which governs the whole evolution of the new agegraphic dark energy model.

Here we consider the noninteracting case for numerical computations because it is a tedious calculation to explore the whole evolution of this model including the interaction, in contrast to the agegraphic dark energy model. In the case of new agegraphic dark energy model, one finds from Fig. 4 that the whole evolution depends on parameter n critically. If n is less than the critical value $n_c \sim 2.6878$, then its far past behavior is not acceptable because of $w_n, v_n^2 \rightarrow \infty$ and $\Omega_n \rightarrow 0$ as $x \rightarrow -\infty$. On the other hand, if n is greater than the critical value, then $w_n \rightarrow -1$ and $\Omega_n \rightarrow 0$, while $v_n^2 < -1$ as $x \rightarrow -\infty$. In this case, we expect to have $\Omega_n \propto a^2$. If n approaches the critical value, then $w_n \rightarrow -2/3$ and $\Omega_n \rightarrow 1$ as $x \rightarrow -\infty$. This corresponds to the matter-dominated universe in the far past, predicted by Wei and Cai [16]. However, in the far future we have the convergent results of $\Omega_n \rightarrow 1$, $w_n \rightarrow -1$, $v_n^2 \rightarrow -2/3$, irrespective of n . Here we note that the squared speed is always negative for $n \geq n_c$. Concerning the evolution with respect to the redshift z [29], this corresponds to the evolution of region between $x = 0 (z = 0)$ and $x = -3.045 (z = 20)$ using $x = -\ln(1+z)$. As is shown in Fig. 4, we find quite different pictures for different n beyond this region. Hence the evolution using z covers a part of the whole evolution.

In order to discuss the radiation-dominated universe in the far past, one has to include a radiation matter which satisfies $\dot{\rho}_r + 4H\rho_r = 0$. Then the evolution equations for density parameters are modified as

$$\Omega'_n = \Omega_n[\Omega_r - 3(1 - \Omega_n)w_n], \quad (29)$$

$$\Omega'_r = \Omega_r[3w_n\Omega_r - (1 - \Omega_r)]. \quad (30)$$

Solving these equations numerically, we find the similar graphs in Fig. 5 except the shift of w_n from $-2/3$ to $-1/3$ in the far past. We observe that there exist a critical value $n_c \sim 2.5137752$, which provides $w_n \rightarrow -1/3$ as $x \rightarrow -\infty$. This corresponds to the radiation-dominated universe with $\Omega_r \rightarrow 1$. The squared speed is obtained as

$$v_n^2 = -\frac{\dot{\omega}_n}{3H(1 + \omega_n)} + \omega_n = -\frac{1}{6}[\Omega_r - 3(1 - \Omega_n)w_n] + w_n + \frac{1}{3}. \quad (31)$$

For $n = n_c$, the squared speed leads to $-1/3$ as $x \rightarrow -\infty$. The critical value of $w_n^c = -1/3$ for the radiation-dominated universe can be understood as follows. To have an asymptotic value of $w_n = w_n^c$ at $x = -\infty (a \rightarrow 0)$, we have

$$\Omega_n = \frac{9n^2}{4}(1 + w_n^c)^2 e^{2x}. \quad (32)$$

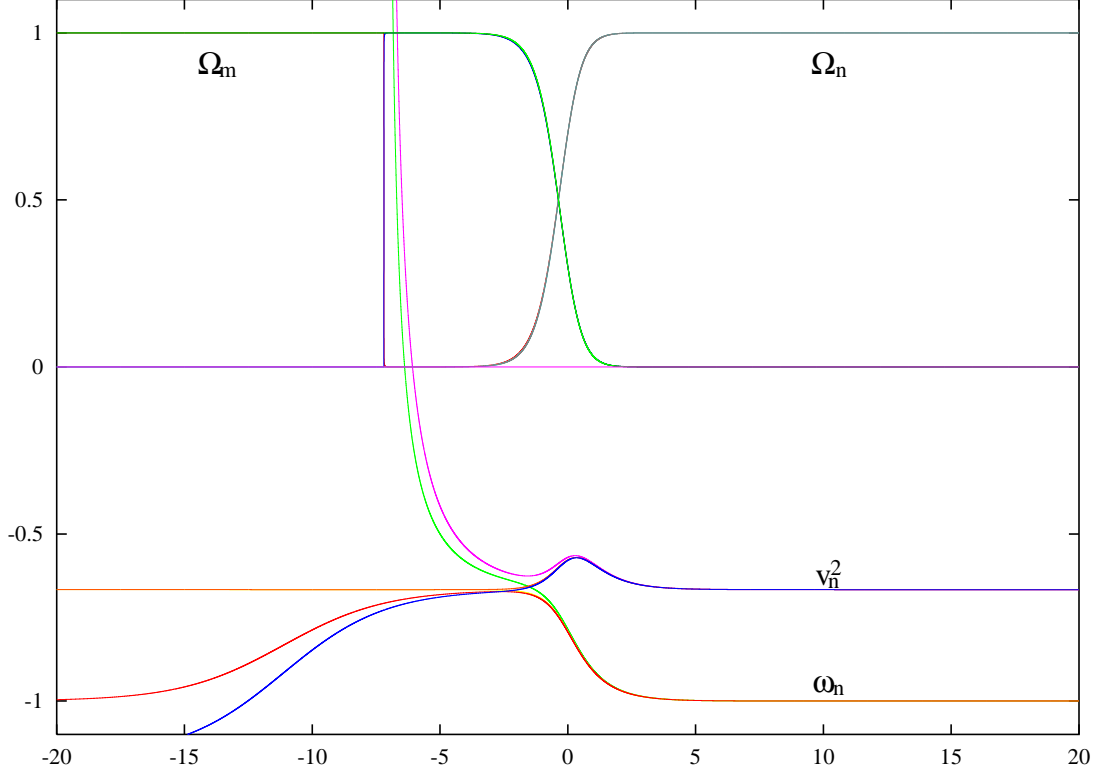


Figure 4: Graphs for the whole evolution of the new agegraphic dark energy. From top to down, the density parameters $\Omega_n(\Omega_m)$, the squared speed v_n^2 , and the EOS ω_q are depicted. Each graph is composed of different n values, $n = 2.6, 2.6878, 2.7$. One distinguishes difference for different n in the region of $x < 0$ and the upper curve in each graph corresponds to smaller value of $n = 2.6$.

Substituting this into Eq.(29), one gets

$$\Omega_r - 3 \left[1 - \frac{9n^2}{4} (1 + w_n^c)^2 e^{2x} \right] w_n^c = 2. \quad (33)$$

Taking the limit of $x \rightarrow -\infty$, we find w_n^c as

$$w_n^c = \frac{\Omega_r - 2}{3}. \quad (34)$$

It gives $w_n^c = -1/3$ for $\Omega_r = 1$ (radiation-dominated era) and $w_n^c = -2/3$ for $\Omega_r = 0$ (matter-dominated era).

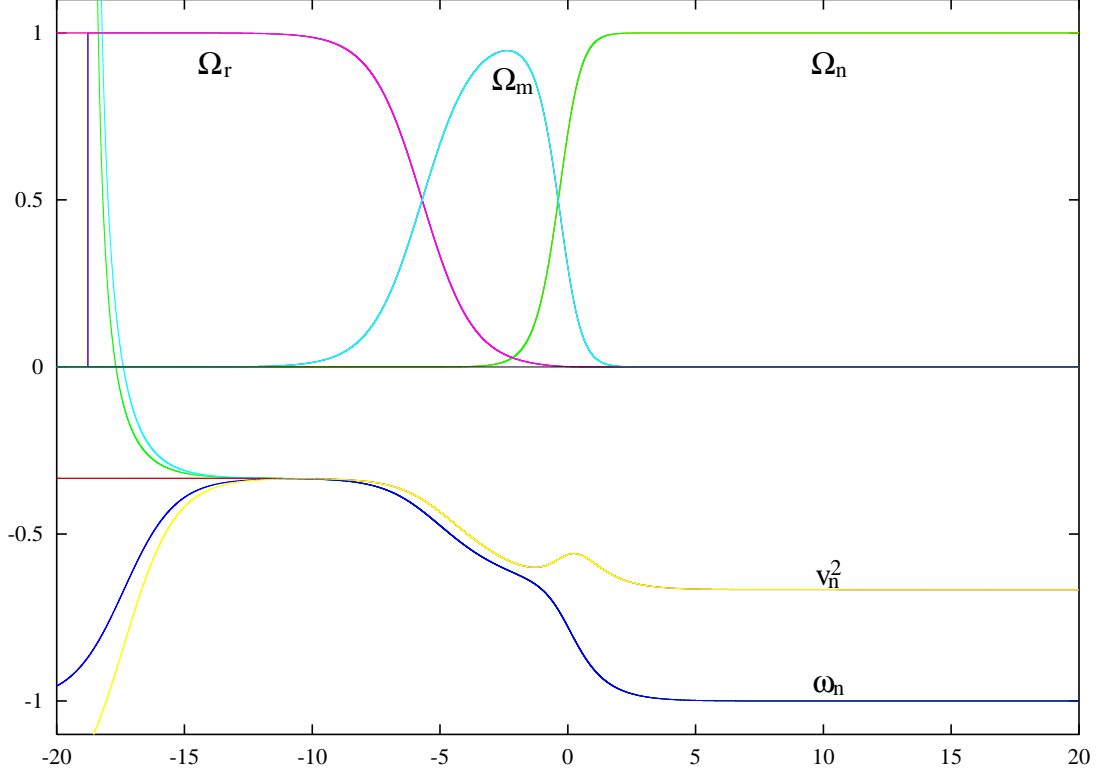


Figure 5: Graphs for the whole evolution of the new agegraphic dark energy. From top to down, the density parameters Ω_n (Ω_m, Ω_r), the squared speed v_n^2 , and the EOS ω_q are depicted. Each graph is composed of different n , $n = 2.513775, 2.513775196, 2.513776$. One distinguishes difference for different n in the region of $x < 0$ and the upper curve in each graph corresponds to smaller value of $n = 2.513775$.

3.2 Interacting case

We extend the new agegraphic dark energy model to include the interaction with the cold dark matter through the continuity equations as

$$\dot{\rho}_n + 3H(\rho_n + p_n) = -Q, \quad \dot{\rho}_m + 3H\rho_m = Q, \quad (35)$$

which shows decaying of new agegraphic dark energy density into the cold dark matter with decay rate $\Gamma = Q/\rho_n$. In this case, the evolution equation takes the form

$$\Omega'_n = \Omega_n \left[-3(1 - \Omega_n) \left(-1 + \frac{2e^{-x}}{3n} \sqrt{\Omega_n} \right) - \frac{Q}{3m_p^2 H^3} \right]. \quad (36)$$

Here we obtain the native equation of state [16]

$$\omega_n = -1 + \frac{2e^{-x}}{3n} \sqrt{\Omega_n} - \frac{Q}{3H\rho_n}. \quad (37)$$

Table 1: Comparison between new agegraphic dark energy model (NADEM) and holographic dark energy model (HDEM) with the future event horizon. Far past means $a \rightarrow 0(x \rightarrow -\infty)$, while Far future denotes $a \rightarrow \infty(x \rightarrow \infty)$. MDU (DEDU) means matter-dominated universe of $\Omega_m \rightarrow 1$ (dark energy-dominated universe of $\Omega_q \rightarrow 1$).

	NADEM	HDEM	Remark
Far past	$\omega_n = -\frac{2}{3}(v_n^2 = 0)$ for $n = n_c$	$\omega_\Lambda = v_\Lambda^2 = -\frac{1}{3}$ for all c	MDU
Far future	$\omega_n = -1(v_n^2 = -\frac{2}{3})$ for all n	$\omega_\Lambda = v_\Lambda^2 = -1$ for $c = 1$	DEDU

The squared speed is given by

$$v_n^2 = \frac{\dot{\omega}_n}{-3H(1 + \omega_n^{\text{eff}})} + \omega_n, \quad (38)$$

where

$$\dot{\omega}_n = \frac{\Omega'_n}{3n\sqrt{\Omega_n}} - \frac{2e^{-x}}{3n}\sqrt{\Omega_n} - \left(\frac{Q}{3H\rho_n}\right)' \text{ and } \omega_n^{\text{eff}} = \omega_n + \frac{Q}{3H\rho_n}. \quad (39)$$

If the decay rate is chosen to be $\Gamma = 3\alpha H$ with $\alpha \geq 0$, one finds an interacting picture. The evolution of the native EOS and the squared speed are similar to the case in Fig. 4 except that all equation of states may include the phantom phase with $\omega_n < -1$.

However, if we introduce the effective equation of state

$$\omega_n^{\text{eff}} = -1 + \frac{2e^{-x}}{3n}\sqrt{\Omega_n}, \quad (40)$$

the squared speed is given by

$$v_n^2 = \frac{\dot{\omega}_n^{\text{eff}}}{-3H(1 + \omega_n^{\text{eff}})} + \omega_n^{\text{eff}}, \quad (41)$$

where

$$\dot{\omega}_n^{\text{eff}} = \frac{\Omega'_n}{3n\sqrt{\Omega_n}} - \frac{2e^{-x}}{3n}\sqrt{\Omega_n}. \quad (42)$$

We expect that the evolution of the effective EOS may be free from the phantom phase. It is conjectured that negative squared speeds may appear in the whole evolution of the universe. Hence the new agegraphic dark energy model may persist in having the negative squared speed, even for including the interaction with the cold dark matter.

4 Discussions

We investigate the agegraphic dark energy model and new agegraphic dark energy model. For this purpose, we calculate their equation of states and squared speeds of sound . We

find that the squared speed for agegraphic dark energy is always negative. This means that the perfect fluid for agegraphic dark energy is classically unstable. Furthermore, it is shown that the new agegraphic dark energy model could describe the matter (radiation)-dominated universe in the far past only when the parameter n is chosen to be $n > n_c$ where the critical value is determined by $n_c = 2.6878(2.5137752)$ numerically.

As is summarized in Table I, if one considers the far past as the matter-dominated universe, there is a slight difference in their EOS of dark energy sector. However, this difference is meaningless because the role of dark energy sector is not important in the far past of matter-dominated universe. In the far future, both evolve toward the dark energy-dominated universe. The difference is that for new agegraphic dark energy model, one has $\omega_n \rightarrow -1$ for all n , while for holographic dark energy model, one has $\omega_\Lambda \rightarrow -1$ for $c = 1$ only. However, this compensates the far past behavior: for new agegraphic dark energy model, one has $\omega_n \rightarrow -2/3$ for $n_c = 2.6878$, while for holographic dark energy model, one has $\omega_\Lambda \rightarrow -1/3$ for all c .

Concerning the squared speed, we find $-2/3 \leq v_n^2 \leq 0$ for new agegraphic dark energy model with $n = n_c$, while for holographic dark energy model with $c = 1$, its range is $-1/3 \leq v_n^2 \leq -1$. Hence, for these cases, we always have the negative squared speed, showing the instability of their fluid models.

In conclusion, the new agegraphic dark energy model is no better than the holographic dark energy model for the description of the dark energy-dominated universe, even though it resolves the causality problem.

Acknowledgment

K. Kim and H. Lee were in part supported by KOSEF, Astrophysical Research Center for the Structure and Evolution of the Cosmos at Sejong University. Y. Myung was in part supported by the Korea Research Foundation (KRF-2006-311-C00249) funded by the Korea Government (MOEHRD).

References

- [1] A. G. Riess *et al.*, *Astron. J.* **116** (1998) 1009 [astro-ph/9805201]; S. J. Perlmutter *et al.*, *Astrophys. J.* **517** (1999) 565 [astro-ph/9812133]; A. G. Riess *et al.*, *Astrophys. J.* **607** (2004) 665 [astro-ph/0402512]; P. Astier *et al.*, *Astron. Astrophys.* **447** (2006) 31 [arXiv:astro-ph/0510447].

- [2] M. Tegmark *et al.* [SDSS Collaboration], Phys. Rev. D **69** (2004) 103501 [arXiv:astro-ph/0310723];
K. Abazajian *et al.* [SDSS Collaboration], Astron. J. **128** (2004) 502 [arXiv:astro-ph/0403325];
K. Abazajian *et al.* [SDSS Collaboration], Astron. J. **129** (2005) 1755 [arXiv:astro-ph/0410239].
- [3] H. V. Peiris *et al.*, Astrophys. J. Suppl. **148** (2003) 213 [astro-ph/0302225]; C. L. Bennett *et al.*, Astrophys. J. Suppl. **148** (2003) 1[astro-ph/0302207]; D. N. Spergel *et al.*, Astrophys. J. Suppl. **148** (2003) 175[astro-ph/0302209].
- [4] D. N. Spergel *et al.*, arXiv:astro-ph/0603449.
- [5] U. Seljak, A. Slosar and P. McDonald, arXiv:astro-ph/0604335.
- [6] E. J. Copeland, M. Sami and S. Tsujikawa, arXiv:hep-th/0603057.
- [7] A. Upadhye, M. Ishak, and P. J. Steinhardt, Phys. Rev. D **72** (2005) 063501[arXiv:astro-ph/0411803].
- [8] M. Li, Phys. Lett. B **603** (2004) 1[arXiv:hep-th/0403127].
- [9] R. G. Cai, arXiv:0707.4049 [hep-th].
- [10] A. Cohen, D. Kaplan, and A. Nelson, Phys. Rev. Lett. **82** (1999) 4971[arXiv:hep-th/9803132].
- [11] Y. S. Myung, Phys. Lett. B **610** (2005) 18 [arXiv:hep-th/0412224].
- [12] F. Károlyházy, Nuovo Cim. A **42** (1966) 390.
- [13] Y. J. Ng and H. Van Dam, Mod. Phys. Lett. A **9** (1994) 335.
- [14] N. Sasakura, Prog. Theor. Phys. **102** (1999) 169 [arXiv:hep-th/9903146].
- [15] M. Maziashvili, Phys. Lett. B **652** (2007) 165 [arXiv:0705.0924 [gr-qc]].
- [16] H. Wei and R. G. Cai, arXiv:0708.0884 [astro-ph].
- [17] S. D. Hsu, Phys. Lett. B **594** (2004) 13[arXiv:hep-th/0403052].
- [18] Q. G. Huang and M. Li, JCAP **0408** (2004) 013 [arXiv:astro-ph/0404229].

- [19] P. J. E. Peebles and B. Ratra, *Rev. Mod. Phys.* **75** (2003) 559 [arXiv:astro-ph/0207347].
- [20] V. Gorini, A. Kamenshchik, U. Moschella, V. Pasquier and A. Starobinsky, *Phys. Rev. D* **72** (2005) 103518 [arXiv:astro-ph/0504576].
- [21] H. Sandvik, M. Tegmark, M. Zaldarriaga and I. Waga, *Phys. Rev. D* **69** (2004) 123524 [arXiv:astro-ph/0212114].
- [22] Y. S. Myung, *Phys. Lett. B* **652** (2007) 223 [arXiv:0706.3757 [gr-qc]].
- [23] H. Kim, *Mon. Not. Roy. Astron. Soc.* **364** (2005) 813 [arXiv:astro-ph/0408577].
- [24] B. Wang, Y. g. Gong and E. Abdalla, *Phys. Lett. B* **624** (2005) 141 [arXiv:hep-th/0506069].
- [25] H. Wei and R. G. Cai, arXiv:0707.4052 [hep-th]; H. Wei and R. G. Cai, arXiv:0707.4526 [gr-qc];
- [26] D. Pavon and W. Zimdahl, *Phys. Lett. B* **628** (2005) 206 [arXiv:gr-qc/0505020].
- [27] H. Kim, H. W. Lee and Y. S. Myung, *Phys. Lett. B* **632** (2006) 605 [arXiv:gr-qc/0509040];
- [28] M. S. Berger and H. Shojaei, *Phys. Rev. D* **73** (2006) 083528 [arXiv:gr-qc/0601086].
- [29] H. Wei and R. G. Cai, arXiv:0708.1894 [astro-ph].
- [30] X. Wu, Y. Zhang, H. Li, R. G. Cai and Z. H. Zhu, arXiv:0708.0349 [astro-ph]; Y. Zhang, H. Li, X. Wu, H. Wei and R. G. Cai, arXiv:0708.1214 [astro-ph].
- [31] I. P. Neupane, arXiv:0708.2910 [hep-th].